

Supplementary Material for “Filling-Factor Dependent Magnetophonon Resonance in Graphene Investigated By High-Field Raman Spectroscopy

Y. Kim¹, J.M.Poumirol¹, A.Lombardo², N. G. Kalugin³, T.Georgiou⁴, Y. J. Kim⁴,
K. S. Novoselov⁴, A. C. Ferrari², J. Kono⁵, O. Kashuba⁶, V. I. Fal’ko^{7,8}, D. Smirnov^{1*}

¹National High Magnetic Field Laboratory, Tallahassee, FL 32310, USA

²Cambridge Graphene Centre, Cambridge University, Cambridge, CB3 0FA, UK

³Department of Materials and Metallurgical Engineering, New Mexico Tech, Socorro, NM 87801, USA

⁴School of Physics & Astronomy, University of Manchester, Oxford Road, Manchester M13 9PL, UK

⁵Department of Electrical and Computer Engineering and Department
of Physics and Astronomy, Rice University, Houston, TX 77005, USA

⁶Institute for Theoretical Physics A, RWTH Aachen, D-52074 Aachen, Germany

⁷Department of Physics, Lancaster University, Lancaster, LA1 4YB, UK and

⁸DPMC, Université de Genève, CH-1211 Genève 4, Switzerland

I: SAMPLE FABRICATION

Large area graphene films are grown on copper foils by chemical vapor deposition (CVD)[1–3]. A $\sim 25\mu\text{m}$ thick piece of Cu foil is initially cleaned with acetone, deionized (DI) water, and isopropanol to remove organic and inorganic contaminants from the surface. The foil is then loaded in a 4 inch quartz tube, and annealed at 1000°C for 30mins with an H_2 flow of 20 cubic centimeters per minute (sccm) and a pressure of 200mTorr. Such annealing process increases Cu grain size and removes native oxide layer. For the growth of graphene films, a gas mixture of H_2 and CH_4 (flow rates of 40 and 20sccm respectively) is injected in the CVD chamber for 30mins while maintaining the pressure at 600mTorr and temperature at 1000°C . Finally, the sample is rapidly cooled to room temperature under a hydrogen flow at a pressure of 200mTorr. Such procedure results in high quality single layer graphene (SLG) growing on both sides of the foil, as shown by Raman spectroscopy[4, 5]. A layer of Poly(methyl methacrylate) (PMMA) is then spun on one of the surfaces of the Cu foil. The graphene layer on the other side of Cu is removed with an oxygen plasma at a pressure of 20mTorr and a power of 10W for 30s. The PMMA/graphene membrane is then released by dissolving the Cu in a 0.2M aqueous solution of ammonium persulphate. The remaining PMMA/graphene layer is cleaned several times by DI water to remove residual salt, and transferred onto the SiO_2/Si substrates. After the sample is dried in ambient conditions, the PMMA is removed in acetone, leaving the graphene adhered to SiO_2/Si [2].

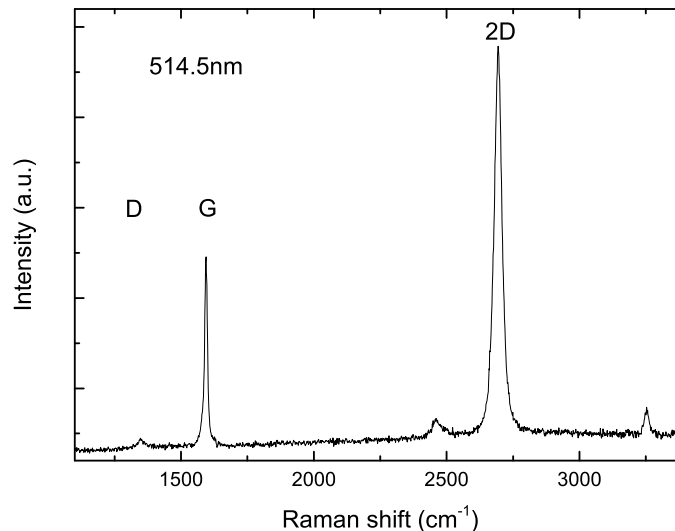


FIG. S1: Raman spectrum measured at 514nm of transferred SLG on SiO_2/Si

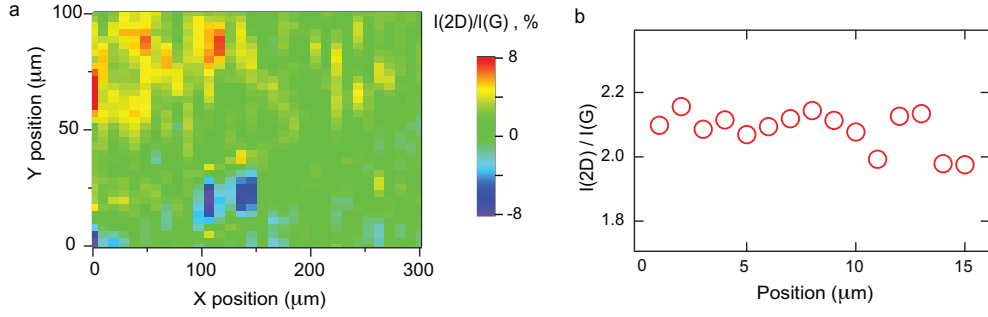


FIG. S2: Raman map (a) and linescan (b), of $I(2D)/I(G)$ for 532nm excitation

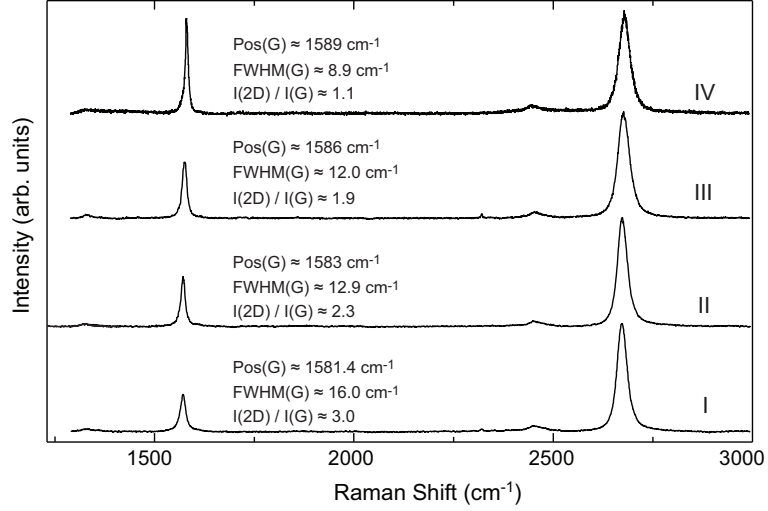


FIG. S3: Raman spectra for SLG I) annealed in Ar/H₂ (8h, 220°C), degassed, exposed to ~1mbar N₂; II) annealed in Ar/H₂ (8h, 220°C), degassed and kept below 10⁻⁴ bar; III) exposed to air for several days; IV) exposed to air for several months

II. RAMAN CHARACTERIZATION

The samples are first measured at 514nm in a Renishaw MicroRaman system. Fig.S1 plots a representative spectrum. This shows a small D peak, and D to G height ratio, $I(D)/I(G) \sim 0.072$. From Ref.5 we estimate a defect density $\sim 2 \times 10^{10} \text{cm}^{-2}$. The sample has ratio of 2D to G peak heights, $I(2D)/I(G) \sim 2$, and a corresponding area ratio, $A(2D)/A(G) \sim 6$. The full width at half maximum of the G peak, $\text{FWHM}(G)$, is $\sim 13 \text{cm}^{-2}$, while the G peak position, $\text{Pos}(G)$, is $\sim 1594 \text{cm}^{-1}$. From these we estimate [6–9] a p-doping $\sim 200 \text{meV}$ and a carrier concentration $\sim 5 \times 10^{12} \text{cm}^{-2}$.

Spatially-resolved Raman measurements are performed in ambient air on the sample attached to a stack of x-y-z piezoelectric stages (Attocube). Fig.S2 shows a Raman map acquired with $\sim 7 \mu\text{m}$ steps using 532nm, $\sim 4 \text{mW}$ excitation focused to a $\sim 10 \mu\text{m}$ spot, as well as a linescan of $I(2D)/I(G)$ measured with $\sim 1 \mu\text{m}$ steps at approximately the same location as probed in the magneto-Raman experiment. The $I(2D)/I(G)$ variation across randomly selected $\sim 10 \mu\text{m}$ spots is typically between 10% and 20%.

Our magneto-Raman set up only accepts 532nm excitation, since one cannot operate 514nm Ar⁺ lasers close to high field magnets. Given that most correlations between doping and Raman spectra were derived at 514nm [6–9], and given that $I(2D)/I(G)$ and $A(2D)/A(G)$ change with excitation wavelength [4, 5, 9], it is important to consider how much the spectra change between 514 and 532nm excitation. By comparing several points measured at these two wavelengths, we do not detect more than 10% variation. We thus consider safe to use 532nm to derive the doping estimates, while Ref.5 provided a correlation between $I(D)/I(G)$ and defect density applicable at any wavelength.

Fig.S3 plots the zero-field Raman spectra measured with 532nm excitation for four different carrier densities, while

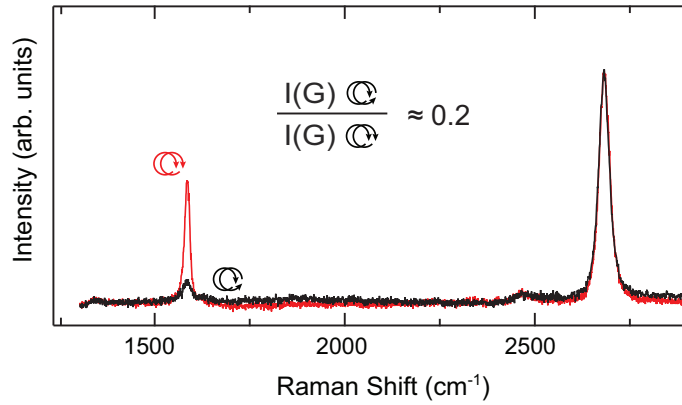


FIG. S4: Raman spectra for (Red) parallel and (Black) crossed circular polarizations of incident and scattered light

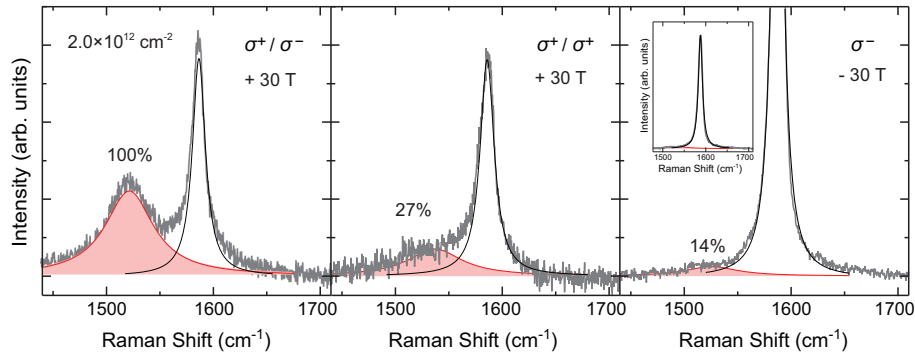


FIG. S5: Polarization efficiency estimated from circular-polarized magneto-Raman spectra measured at 30T on SLG at intermediate carrier density.

the corresponding magneto-Raman spectra are discussed in the main text. Under ambient laboratory conditions, the SLG sample is initially p-doped with a carrier concentration $\sim 5 \times 10^{12} \text{cm}^{-2}$. By adjusting annealing parameters (typically 8 hours in 90%/10% Ar/H₂ atmosphere at temperatures up to 220°C) and degassing in $< 10^{-4}$ mbar vacuum, the sample can be made n-type, with an electron density $\sim 2 \times 10^{12} \text{cm}^{-2}$. Exposing the sample to low-pressure (~ 1 mbar or less) N₂ atmosphere reduces the carrier density to $\sim 0.4 \times 10^{12} \text{cm}^{-2}$. The exposure to ambient pressure N₂ gas or air results in hole doping, restoring p-type doping with carrier densities $\sim (5-6) \times 10^{12} \text{cm}^{-2}$. If the sample is left in ambient air for a long period of time, it continues to experience p-doping reaching a carrier concentration $\geq 10^{13} \text{cm}^{-2}$ in several weeks. However, this doping is inhomogeneous, with a 10 to 20% variation, as shown by Raman mapping.

Most of the magneto-Raman data in the main text are measured with circularly polarized light. Thus, it is essential to analyze the polarization efficiency of our setup. This is defined as the ratio of the amount of light transmitted through two circular polarizers with parallel or crossed helicities. Field-dependent Raman measurements are performed using a magneto-optical insert, as for Ref.10, equipped with circular polarizers. Each circular polarizer consists of a linear polarizer and an aligned quarter waveplate. To test the polarization efficiency of the excitation light, the second polarizer (analyzer) is installed at the sample position. The ratio of transmitted power of 532nm light in crossed and parallel circular polarizations is $\sim 10\%$. The I(G) ratio measured in crossed and parallel polarizations allows us to estimate the total polarization efficiency at the wavelength corresponding to $\sim 1580 \text{cm}^{-1}$ (Fig.S4). In order to estimate the polarization efficiency over the broad range of frequencies interested by the magneto-phonon resonance anti-crossing discussed in the main text, we need to further consider the wavelength dependence of optical retardation in our quarter waveplates, which gives an additional depolarization. We thus estimate that the average depolarization of the scattered light in the $\sim 1450-1700 \text{cm}^{-1}$ spectral range is $\sim 25\%$. These estimates are consistent with the polarization efficiency extracted from the ratios of the MPR sideband intensities measured at 30T on the sample with intermediate carrier density (see Fig.S5). The limited polarization selectivity and doping level inhomogeneities blur the two-component MPR at $\nu < 2$. The presence of two spectral components can be evidenced by plotting the second derivatives of the Raman spectra (Fig.S6).

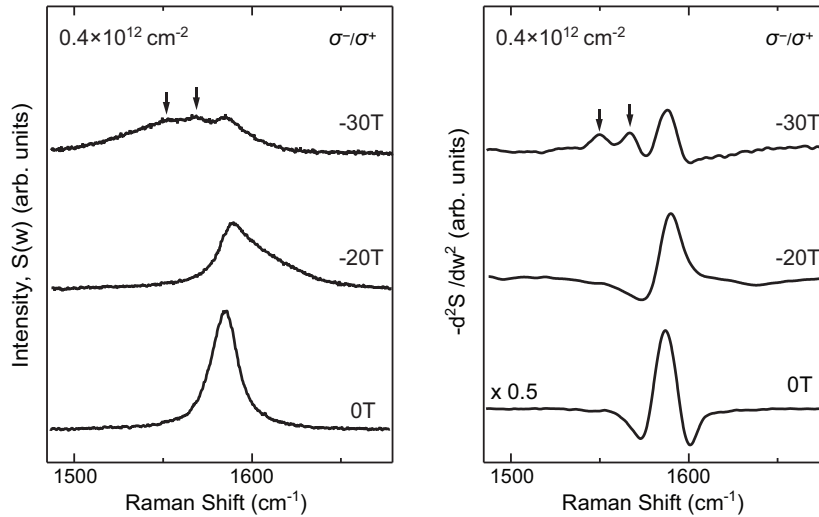


FIG. S6: Two high-field MPR sidebands (indicated by arrows) resolved in cross-polarized magneto-Raman spectra measured on SLG at intermediate carrier density.

* Electronic address: smirnov@magnet.fsu.edu

- [1] X. Li et al. *Science* **324**, 1312 (2009)
- [2] S. Bae et al. *Nature Nanotech.* **5**, 574 (2010)
- [3] F. Bonaccorso *et al.*, *Materials Today* **15**, 564 (2012)
- [4] A. C. Ferrari et al. *Phys. Rev. Lett.* **97**, 187401 (2006)
- [5] L.G. Cancado et al. *Nano Lett.* **11**, 3190 (2011)
- [6] A. Das et al. *Nature Nanotech.* **3**, 210 (2008)
- [7] S. Pisana et al. *Nature Mater.* **6**, 198 (2007)
- [8] C. Casiraghi et al. *Appl. Phys. Lett.* **91**, 233108 (2007)
- [9] D. M. Basko et al. *Phys. Rev. B.* **80**, 165413 (2009).
- [10] Y. Kim *et al.*, *Phys. Rev. B* **85**, 121403(R) (2012).